

Mobilities of carbon cluster ions: Critical importance of the molecular attractive potential

Alexandre A. Shvartsburg, George C. Schatz, and Martin F. Jarrold

Department of Chemistry, Northwestern University, 2145 Sheridan Road, Evanston, Illinois 60208

(Received 26 June 1997; accepted 31 October 1997)

Mobilities in helium gas for isomers belonging to the major structural families of carbon clusters identified in drift tube studies (chains, monocyclic and bicyclic rings, graphite sheets, and fullerenes and their dimers) have been evaluated by trajectory calculations employing a realistic ion-He interaction potential. For all the species considered, the agreement between the measured and calculated mobilities at room temperature improves by at least a factor of 3 over that obtained with the widely used hard-sphere projection approximation. Furthermore, for a large representative sample of clusters belonging to all the above families, the results of trajectory calculations as a function of temperature over the range of 78–360 K are in a good agreement with the measured mobilities. This shows that the C–He pairwise potential is only weakly dependent on the structure and chemical bonding of a carbon cluster. Thus this study demonstrates the universal suitability of trajectory calculations for the accurate prediction of the gas phase mobilities for polyatomic ions with various shapes and sizes, and the uniform superiority of this method over the previously used approximations. In particular, the trajectory calculations for large ($n=120$ –140) fullerenes show that these cages have near-spherical shapes found by theory, while the projection approximation would erroneously assign them as “buckytubes.” It also appears that the mobility may be substantially affected by the degree of charge localization on a specific atom in the cluster, especially at low temperatures. © 1998 American Institute of Physics. [S0021-9606(98)50706-4]

I. INTRODUCTION

Since the first application of ion mobility measurements^{1,2} to the structural elucidation of atomic clusters,³ most studies have focused on carbon clusters, either pure^{3–14} or doped by other elements.^{15–24} This research has revealed a great diversity in the geometries of gas phase carbon clusters, including chains, monocyclic, bicyclic, and polycyclic rings, graphite sheets, and fullerene monomers and oligomers. Similar structural families have been observed for carbon clusters doped by atoms of metals,^{15–20,23} semiconductors,²¹ halogens,²² and hydrogen.²⁴

The technique of ion mobility measurements is based on the fact that isomers of differing shapes travel with different velocities when dragged through a buffer gas by an electric field, and thus can be separated from each other.¹ The resolved peaks are assigned by matching the experimental mobilities with values calculated for candidate geometries. While a wealth of knowledge about the general shapes of various polyatomic ions has been obtained in such studies, detailed structural information has often been elusive. The major cause of this situation is that, with existing theories, the overall quality of fits to the measured mobilities for polyatomic ions has remained wanting. For example,^{5,6} the peaks for some carbon cluster isomers deviate from their expected positions by more than 10%. Since agreement with the calculated mobility of a trial geometry within 2% has been introduced as a criterion for the assignment of experimental features,^{6,23,25} deviations of this magnitude are clearly unacceptable. Recently, high-resolution ion mobility measurements²⁶ have achieved a resolution of <0.7%,

which is over a factor of 10 improvement over the prior state of the art. This advance has shifted the degree of agreement normally found between the experimental and calculated mobilities from mostly tolerable to unsatisfactory. Hence the precision of mobility calculations, rather than the resolving power, has now become the principal limiting factor in ion mobility measurements.

The experimental mobilities for polyatomic ions, including carbon clusters, have been previously analyzed by the widely accepted hard-sphere projection approximation.^{5–20,22–24,27–31} originally introduced by Mack.³² We have recently developed the computational tools to evaluate the gas phase mobility of a polyatomic ion by propagating trajectories which simulate its collisions with buffer gas atoms in a realistic intermolecular potential.³³ This approach has been proven superior to the projection approximation in fitting the mobilities in He for a number of fullerenes containing up to $n=240$ atoms.³³ We have also found that the projection approximation leads to the wrong structural assignments for fullerene dimers, and that trajectory calculations have to be performed if the correct assignments are to be made.³⁴ All modeling has employed a pairwise additive Lennard-Jones (LJ) potential plus a charge-induced dipole term with the charge uniformly delocalized over all cluster atoms.^{33–35} The LJ parameters for this potential ($\sigma=3.043$ Å and $\epsilon=1.34$ meV for the C–He interaction, where ϵ is the depth and σ is the distance where the potential becomes positive) were fit to reproduce the measured mobilities for a C_{60}^+ fullerene over an 80–400 K temperature range.^{33,34} This potential is essentially equivalent to that ob-

tained using combination rules³⁶ ($\sigma = 3.03 \text{ \AA}$ and $\epsilon = 1.40 \text{ meV}$) and correlates reasonably well with those extracted from He scattering on bulk graphite surfaces.³³ However, no data as a function of temperature have been obtained for any other carbon cluster ions, hence the critical issue of the transportability of the C–He potential to other species remained unclear. As the ultimate test of our model is its performance for all carbon cluster ions at all temperatures, we have extended the temperature-dependent mobility measurements and trajectory calculations to the other major isomer families identified in the drift tube studies of cations or anions: chains, mono- and bicyclic rings, and graphite sheets.

II. EXPERIMENTAL TECHNIQUES

The mobilities of the cluster cations were measured using the tandem quadrupole drift tube apparatus described in detail elsewhere.³⁷ Briefly, the clusters are generated by pulsed 308 nm laser vaporization of a graphite rod (Ultra Carbon, Ultra F) and entrained in a continuous He gas flow. They are ionized while in this flow using a 1.1 kV electron beam, mass selected, and injected at a controlled energy into a 7.6 cm long drift tube containing He buffer gas. The clusters exiting the drift tube are mass selected one more time and detected by an off-axis collision dynode and dual micro-channel plates. The drift tube can be cooled down to 78 K using liquid nitrogen or heated by electric heaters. The temperature is monitored by four thermocouples installed along the drift tube. The average of four values was recorded, with the gradient being below 3 K. The drift field and buffer gas pressure were varied in the ranges of 9.2–15.4 V/cm and 2.5–10 Torr, respectively. These conditions correspond to an E/N of 1.5–10 Td. The measured reduced mobilities were independent of the drift field and buffer gas pressure within the ranges employed. This verifies that the experiments were conducted in the low drift field regime. The injection energy was adjusted over a 50–170 eV range. The measured reduced mobilities were independent of the injection energy. The fact that the mobilities do not depend on the buffer gas pressure or injection energy indicates that the thermalization length following injection is negligible and that the effective length of the drift tube is constant.

In order to achieve the maximum accuracy for the mobility of a specific isomer, the injection energy was often adjusted so that the relative abundance of that isomer was enhanced and/or that of close neighbors diminished.

III. COMPUTATIONAL METHODS

In the limit of low drift field, where the mobility is independent of the field, the reduced mobility is inversely proportional to the orientationally averaged collision integral^{38,39} $\Omega_{\text{avg}}^{(1,1)}$:

$$K = \frac{(18\pi)^{1/2}}{16} \left[\frac{1}{m} + \frac{1}{m_B} \right]^{1/2} \frac{ze}{(k_B T_{\text{EF}})^{1/2}} \frac{1}{\Omega_{\text{avg}}^{(1,1)}} \frac{1}{N}. \quad (1)$$

Here m and m_B are, respectively, the masses of the ion and of the buffer gas atom, N is the buffer gas number density, ze is the ionic charge, and T_{EF} is the effective gas temperature;³⁸ $T_{\text{EF}} = T + m_B \nu_D^2 / 3k_B$, where T is the buffer

gas temperature and ν_D is the drift velocity.⁴⁰ The quantity $\Omega_{\text{avg}}^{(1,1)}$ should be evaluated by numerically integrating the momentum transfer cross section over the Maxwellian distribution of relative velocities (at the temperature T_{EF}) between the buffer gas atom and the ion. This cross section is determined by averaging a function of the scattering angle χ over the impact parameter b and the collision geometry determined by angles θ , φ , and γ . The above procedure is implemented in our classical trajectory calculations³³ by means of the integral

$$\begin{aligned} \Omega_{\text{avg}}^{(1,1)} = & \frac{1}{8\pi^2} \int_0^{2\pi} d\theta \int_0^\pi d\varphi \sin \varphi \int_0^{2\pi} d\gamma \frac{\pi}{8} \left(\frac{\mu}{k_B T} \right)^3 \\ & \times \int_0^\infty dg e^{-\mu g^2 / (2k_B T)} g^5 \int_0^\infty 2bdb(1 \\ & - \cos \chi(\theta, \varphi, \gamma, g, b)), \end{aligned} \quad (2)$$

where μ is the reduced mass of the ion and buffer gas atom and g is their relative velocity. Our treatment assumes fully elastic collisions and rigid nonrotating ions. A more sophisticated model, that includes energy exchange between the translational and rotational degrees of freedom during the collision, has been constructed by Viehland and Dickinson.⁴¹ However, its application has been limited to diatomic ions.^{41,42}

The simple projection approximation^{6,32,43} totally ignores all the details of the scattering process between the ion and the buffer gas by replacing the average collision integral in Eq. (1) with the average geometric cross section:

$$\begin{aligned} \Omega_{\text{avg}}^{(1,1)} = & \frac{1}{4\pi} \int_0^{2\pi} d\theta \int_0^\pi d\varphi \sin \varphi \int_0^{2\pi} d\gamma \\ & \times \int_0^\infty bdb M(\theta, \varphi, \gamma, b), \end{aligned} \quad (3)$$

where an integer-valued function M is unity when a hard-sphere collision occurs for a geometry defined by θ , φ , γ , and b , and null otherwise. For contiguous bodies, Eq. (3) is equivalent to familiar

$$\begin{aligned} \Omega_{\text{avg}}^{(1,1)} & \approx \frac{1}{8\pi^2} \int_0^{2\pi} d\theta \int_0^\pi d\varphi \sin \varphi \int_0^{2\pi} d\gamma \pi b_{\text{min}}^2(\theta, \varphi, \gamma), \end{aligned} \quad (4)$$

where b_{min} is the minimum impact parameter for a collision geometry defined by θ , φ , and γ that avoids a hard-sphere contact with any atom in the cluster. This obviously ignores the attractive interactions between the ion and buffer gas atoms and the multiple reflections on the ion surface. Recently, two of us developed an exact hard-sphere scattering model which rigorously includes the details of the scattering process under the assumption of a hard sphere C–He interatomic potential.⁴⁴ This reduces Eq. (2) to

$$\begin{aligned} \Omega_{\text{avg}}^{(1,1)} = & \frac{1}{4\pi} \int_0^{2\pi} d\theta \int_0^\pi d\varphi \sin \varphi \int_0^{2\pi} d\gamma \\ & \times \int_0^\infty bdb(1 - \cos \chi(\theta, \varphi, \gamma, b)). \end{aligned} \quad (5)$$

The computational requirements of our trajectory calculations³³ scale roughly in proportion to $n^{3/2}$ for near-spherical species such as fullerenes, but grow rapidly with the increasing aspect ratio of the cluster and decreasing temperature. This has prevented us from attempting these calculations for chains and monocyclic rings beyond $n=36$ and $n=55$, respectively, while the mobilities for fullerene clusters as large as icosahedral $(C_{60})_{13}$ has been successfully enumerated. All calculations reported here have been converged such that the standard error of the mean is under 0.2%, which in some cases required the propagation of up to 7×10^6 trajectories at an expense of several hundred CPU hours using a top-level workstation.

IV. COMPARISON OF PREDICTED MOBILITIES WITH MEASUREMENTS

In agreement with the literature, for C_n cations we observed chains^{3,4,6,8} for $n \leq 10$, monocyclic rings^{3,4,6,8,9,12} for $n \geq 7$, bicyclic rings from $n \approx 20$ to $n > 40$, graphite sheets¹³ between $n=29$ and $n \approx 70$, and fullerenes for $n \geq 30$. The mobilities for a large sample of structures⁴⁵ belonging to each of these families was measured at temperatures ranging from 78 to 360 K. For mobility calculations, the model geometries for both linear chains and rotationally symmetric monocyclic ring isomers were constructed assuming cumulenic bonding with 1.29 Å for all C=C bond lengths, in close agreement with the results of recent high-level calculations⁴⁶⁻⁴⁹ and spectroscopic data of Saykally and coauthors^{50,51} for neutral chains. Some theoretical studies^{7,49,52-57} concluded that the neutral carbon rings for certain sizes have polyyinic bonding (C-C≡C) with alternating bond lengths, but their average is still about 1.29 Å as it is in other calculations favoring cumulenic bonding.⁵⁸ We have verified that the mobilities calculated for chains and rings are independent of whether the bond lengths are assumed equal or alternating, as long as their average remains the same.⁵⁹ Geometries for planar bicyclic rings were found⁶⁰ using the strain minimization model of Shelimov *et al.*,¹³ and the graphite sheets and fullerenes were optimized⁶⁰ with MNDO.⁶¹

The results of mobility simulations are compared with the experimental values in Fig. 1 for all chains and in Fig. 2 for selected monocyclic ring, bicyclic ring, graphite sheet, and fullerene clusters (the pattern for other sizes studied was the same). The deviations for small fullerenes are within the combined experimental and computational error ($\sim 1\%$) at any temperature between 78 and 360 K. The deviations for small graphite sheets are only slightly larger, up to $\sim 2\%$, which is excellent considering that the specific structures for these isomers are not known and that a number of energetically close geometries probably coexist. This good agreement for the fullerenes and graphite sheets is perhaps not surprising, since our C-He potential was obtained by fitting mobilities for C_{60} fullerene, and fullerenes and graphite sheets both consist of sp^2 -hybridized carbon atoms. Although the agreement for monocyclic rings and chains made of sp -hybridized carbons should also be considered fairly good, the deviations are larger, up to 4% and 8%, respectively. Note that the trend of the deviations is similar for all

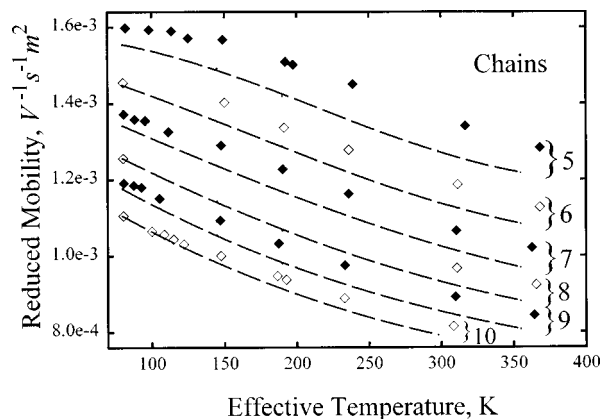


FIG. 1. Mobilities in He for cationic carbon chains ($n=5-10$) as a function of temperature. Diamonds, filled for odd sizes and empty for even, are the experimental data. Mobilities simulated using trajectory calculations are indicated by dashed lines.

cluster sizes and also between the two families: all theoretical curves are slightly steeper than the measured ones while the mobilities tend to be underestimated. Within the framework of our model, this would indicate that the sp C-He potential is slightly shorter-range and deeper than the sp^2 C-He one. To quantify this, we performed calculations using LJ parameters of $\sigma_1=2.93$ Å and $\epsilon_1=1.60$ meV. We found that this modified potential provides an excellent (within 2%) fit to the experimental curves for all monocyclic carbon rings in the size range studied. The picture for bicyclic rings is analogous to that for monocyclic ones: the curves calculated using the original potential are always slightly too steep. The deviations decrease upon the renormalization of the potential as described above, which is satisfying in view of the fact that these rings contain mainly sp -hybridized carbon atoms. However, the quality of agreement for the bicyclic rings does not necessarily confirm the validity of our trajectory calculation model. This is because many unresolved bicyclic ring structures with slightly different mobilities are produced in

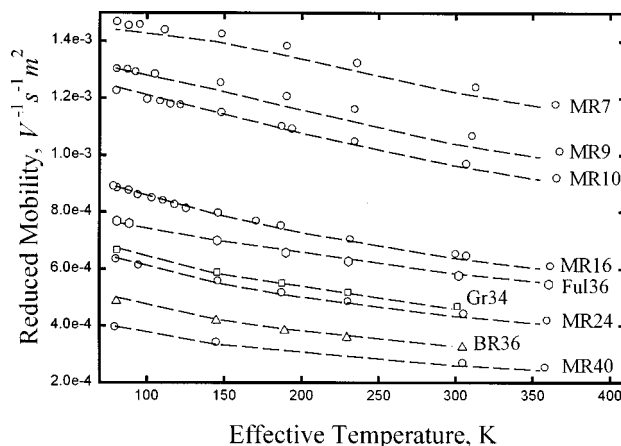


FIG. 2. Mobilities in He for representative carbon cluster cations as a function of temperature. Symbols are the measurements: circles for monocyclic rings ($n=7,9,10,16,24,40$), triangles for a bicyclic ring ($n=36$), squares for a graphite sheet ($n=34$), and hexagons for a fullerene ($n=36$). Dashed lines are the results of trajectory calculations.

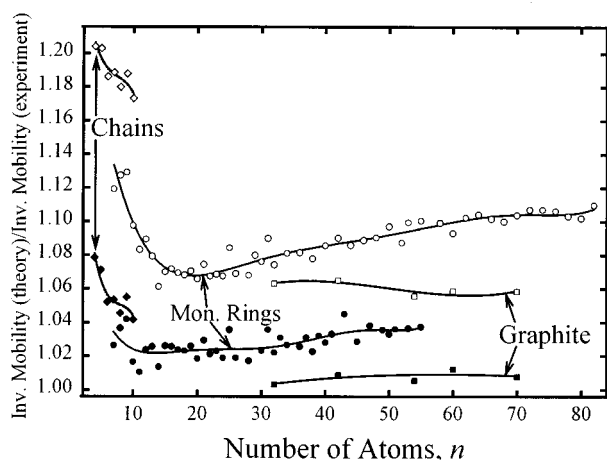


FIG. 3. Relative deviations of the calculated collision integrals for nonfullerene carbon cluster cations from experiment. Chains, monocyclic rings, and graphite sheets are denoted by diamonds, circles, and squares, respectively. Empty and filled symbols represent the predictions of the projection approximation and the trajectory calculations, respectively. Lines are regressions through the data.

the laser vaporization source, as is apparent from the excessive peak width for this isomer.^{6,13}

In Fig. 3 we compare the performance of trajectory calculations with that of the projection approximation in predicting the room-temperature mobilities for carbon cluster cations. A C–He collision radius of 2.86 Å, chosen⁴⁴ to reproduce the mobility of a C₆₀ fullerene at 25 °C, was employed in the projection approximation. The values obtained from trajectory calculations are evidently in a lot better agreement with experiment, for all isomer families, for every cluster size. Specifically, the maximum deviations are reduced from 21% to 8% for chains with $n=4-10$, from 13% to 4% for monocyclic rings with $n=7-55$, and from 7% to 1% for graphite sheets with $n=30-70$; with the average deviations decreasing even more appreciably. The above values correspond to the potential derived by Mesleh *et al.*³³ and used for the evaluations presented in Fig. 3, the deviations for chains and rings decreases still further if the alternative potential for *sp*-bound carbons is used. We emphasize that the errors of the projection approximation for specific isomeric families exhibited in Fig. 3 are not physically meaningful in themselves, because our choice of the C₆₀ fullerene⁴⁴ to fit the collision radius. One could choose a chain instead, in which case the errors would be smallest for chains, greater for the graphite sheets and rings, and the largest for fullerenes. The true indicator of the quality of a model is the total spread between the maximum and minimum errors for all cluster families. For the projection approximation, this spread is about 26% (between $> +21\%$ for chains to -5% for the C₇₀ dimer,³⁴ three times worse than that for the trajectory calculations (between $+8\%$ for chains and 0% for small fullerenes and their dimers).

The trends apparent in Fig. 3 have simple physical explanations. The projection approximation overestimates the cross sections of graphite sheets, monocyclic rings, and chains, the error increasing in this order. Notably, the sequence in which these isomers appear in the arrival time

distributions following the fullerenes is the same. This happens because, as a cluster becomes less compact and its mobility decreases, a He atom can efficiently interact with a smaller number of carbons at a time. This reduces the overall depth of the attractive potential, which lowers the effective hard sphere collision radius. Inspection of Fig. 3 reveals that the substantial across-the-board overestimation of the collision cross sections for noncompact isomers largely disappears in the trajectory calculations treatment. Further, the curve showing the error of the projection approximation for monocyclic rings has a minimum at about $n=20$; in contrast for chains and graphite sheets this error is basically size independent. This minimum for the medium-size rings reflects the enhancement of the measured cross sections by the multiple reflections of He atoms inside the rings. This enhancement was predicted by our exact hard-spheres scattering model⁴⁴ to have a maximum of several percent at $n=20$. The trajectory results, whose relative deviations from the measured mobilities do not go through a comparable minimum (Fig. 3), are consistent with the prediction of that model. When the trajectory calculations are used, the agreement between the drift times of experimental peaks arriving immediately following the fullerenes and the theoretical values for graphite sheets is essentially perfect throughout the whole size range. This fact confirms the assignment of this feature to planar graphite sheets¹³ rather than the three-dimensional rings⁶ or curved carbon sheets containing hexagons and pentagons⁴⁴ (“buckybowls”). The absence of buckybowls among the products formed in cooling carbon plasma is of tremendous significance when weighing the merits of different models for fullerene synthesis,⁶ particularly as related to the “pentagon road.”

V. “BUCKYTUBES,” ANOTHER CASE WHERE THE PROJECTION APPROXIMATION IS MISLEADING

We had previously reported³⁴ that the room-temperature mobility for the $[2+2]$ C₆₀ dimer cation or anion obtained by trajectory calculations is within 0.5% of the measurements. Now we have used trajectory calculations to evaluate the inverse mobility for this dimer (MNDO)⁶¹ geometry of Strout *et al.*⁶² at 80 K as 2800 ± 5 V s/m², in agreement with the experimental value⁶³ of 2780 ± 30 V s/m², for cation. This verifies that our potential is correct for the fullerene dimers and confirms our assignment of these species as $[2+2]$ cycloadducts. The mobility for a $[2+2]$ (C₆₀)₂ at 298 K produced by the projection approximation is in error by over 4%. This would cause an incorrect structural assignment of a stick-bridged geometry.³⁴ This is not an isolated case. The projection approximation also misguides the structural elucidation of large fullerenes.

The room-temperature mobilities measured for the dominant isomers of C₁₂₀ and C₁₄₀ cage cations and anions are in excellent agreement³⁴ with the results of trajectory calculations for the most spherical isomers of these clusters,⁶⁴ D₆ and I_h, respectively, but not with those for the elongated “tubular” geometries.³⁴ For C₁₂₀, this remains the case⁶³ at 80 K. All published calculations (MNDO,^{61,62,65,66} tight binding,⁶⁴ and Hartree–Fock⁶⁶) find the stability of a fullerene cage decreasing with increasing aspect ratio. Con-

TABLE I. Mobilities for the large fullerene ions, experiment and theory. The range of computed values includes both the uncertainty due to the method of geometry optimization and the statistical error margin of calculation.

Geometry			Inverse mobility at 298 K, V s/m ²			
Point group	Reference	Aspect ratio	Projection approximation	Trajectory calculations	Measurement	
C ₁₂₀	D ₆	64	1.0	3530	3630–3635	3610 ± 10
	T _d	62, 64, 66	1.1	3550–3575	3640–3675	
	D _{6d}	62, 64, 66	1.3	3560–3580	3645–3670	
	D _{5d} SF	64, 66	1.5	3560–3580	3635–3670	
	D _{5d} VF	62, 64, 66	2.0	3635–3655	3695–3720	
C ₁₄₀	I _h	64	1.0	3905	4025–4035	4030 ± 10
	D ₅	64	1.8	3985	4080–4090	
	D _{5d}	64	2.4	4085	4155–4170	

versely, the projection approximation suggests⁶⁷ that the experimentally observed fullerenes in the range of $n=100-320$ are all prolate, increasingly so for large sizes. Specifically, the C₁₂₀ and C₁₄₀ cage peaks in the arrival time distributions would be both mistakenly assigned to one of the high-energy elongated “buckytubes” with the aspect ratio of about two (see Table I), and the same would happen for the C₁₃₀. The correct structural characterization of large fullerenes is of crucial importance in understanding the assembly of carbon nanotubes. The hypothesis that, with increasing size, fullerene cages become elongated, and turn into single-walled nanotubes (SWNT) in the gas phase, has been extensively debated.⁶⁶ The analysis of mobility data¹⁴ using the projection approximation would have supported this hypothesis.

VI. IS THE PROBLEM WITH CARBON CHAINS OF DYNAMIC ORIGIN?

The new LJ parameters σ_1 and ϵ_1 described above also substantially improve the agreement with the experiment for chain isomers. Still the mobilities are uniformly underestimated by several percent, particularly (a) at higher temperatures and (b) for chains with an odd number of atoms, regardless of the potential employed. Von Helden *et al.*⁶ have suggested that the cause of the deviations for the chains lies in their thermal motion. Indeed, all polyatomic ions vibrate while drifting through a gas, thus the integrals in Eqs. (2)–(5) should be convoluted over the range of structures sampled as performed by Scuseria and collaborators.²⁹ The thermal motion of carbon chains at moderate temperatures is primarily manifested in their low-frequency bending vibrations around the ground-state linear structure.^{50,51} Any bending of a chain results in a decrease in the cross section, therefore the true time-averaged values must be below our calculated ones, and the difference would increase with increasing temperature. Since it has been established that the rigidity of neutral carbon chains undergoes periodic oscillations as a function of length,^{68,69} it may seem that both features of the deviations from experiment pointed out above can be explained by vibrational dynamics. However, this ef-

fect is not a major cause for the small residual deviations remaining for chains (or rings), for the following two reasons.

(1) We have estimated the magnitude of the dynamic effect for carbon chains by averaging the mobility over a statistical ensemble of bent chains generated by a classical Monte Carlo simulation performed at and above 300 K. This procedure is equivalent to the well-known vibrational sudden approximation in scattering theory. All bond lengths were constrained, and an axially symmetric harmonic bending potential at each carbon atom was assumed with the force constant estimated for the C=C=C bond in carbon rings¹³ (0.83 meV/deg²). Geometries involving spatial overlap of the non-neighboring atoms were prohibited, however, at the temperature of the simulations these were not encountered anyway. Since our interest here is in the relative deviations in mobility from that of straight chains, mobilities were computed using the simple projection approximation. Employing this model, we determined that, even for chains as long as 40 atoms, the average cross section for an ensemble of three-dimensional conformers equilibrated at room temperature is only a fraction of a percent lower than that for the linear geometry, and the difference for chains with less than 10 atoms is too negligible to be identified. These estimations are admittedly quite crude since they use the projection approximation for mobility calculations and allow neither C–C bond stretching nor quantization of vibrational levels in the bending potential. We nonetheless believe that this simplified treatment proves that the dynamic effect is at least an order of magnitude short of explaining the deviations found for small cationic carbon chains. This conclusion is in broad agreement with that previously reached by Scuseria and collaborators²⁹ for monocyclic rings and other carbon cluster isomers.

(2) The relative deviations due to the chain dynamics should increase with increasing chain length, but the trend in Fig. 1 is the opposite, both in the progression of odd $n=5, 7, 9$ and even $n=6, 8, 10$. To further clarify this point, we have investigated the anionic carbon chains which survive to much larger sizes than the cationic ones.^{4,8} Bowers and co-workers^{4,5,8} reported the mobilities of these species up to

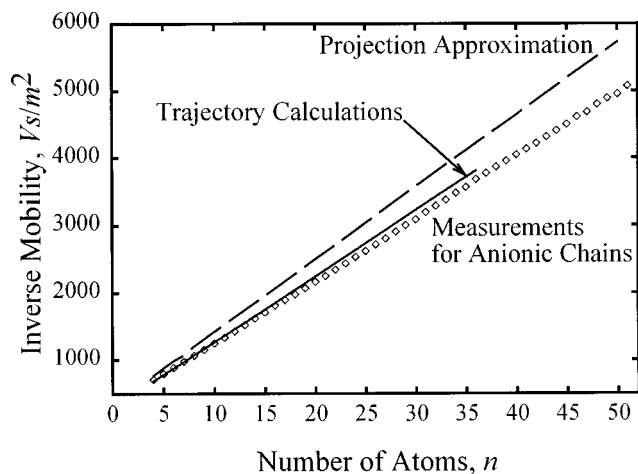


FIG. 4. Inverse mobilities (reduced mobilities⁻¹) for the anionic carbon chains, experiment, and theory.

$n=30$, but could not separate them from the monocyclic rings beyond that because of limited instrumental resolution. Taking advantage of the tenfold improvement in resolving power provided by the new apparatus,²⁶ Dugourd *et al.*⁷⁰ were able to achieve baseline resolution of chain isomers up to $n \sim 50$. The measured room-temperature mobilities are plotted in Fig. 4 along with the values yielded by both the trajectory calculations using the “fullerene” potential³³ and the projection approximation. The far superior performance of the trajectory method is obvious, and the relative residual discrepancy does not appear to increase with increasing chain length beyond $n=20$ which is still another argument against a dynamic cause for the deviations.

VII. INFLUENCE OF CHARGE LOCALIZATION ON IONIC MOBILITY

Continuing the search for the cause of the residual few percent deviations remaining for the carbon chains, we have directed our attention towards the issue of localization of the extra charge on specific cluster atoms. To assess the applicability of our assumption that this charge is uniformly distributed among all atoms, we have modeled the room-temperature mobilities of C_{60}^{+z} and C_{70}^{+z} fullerene ions ($z=1-4$) measured by von Helden *et al.*⁶ (Fig. 5). As the charge increases, the mobilities progressively fall below the linear prediction of a hard-sphere model. This happens because the higher charge deepens the total attractive potential by augmenting its charge-induced dipole component. Our trajectory model fits the experimental data within their uncertainty. This confirms that our treatment of the ionic charge for fullerenes as fully delocalized is appropriate.⁷¹ The good agreement between our calculations and the measurements for the smaller carbon rings suggests that the model is valid for this isomer as well. However, it might be that the assumption of uniform delocalization is suitable for fullerenes and monocyclic rings where all atoms are (nearly) equivalent, but not for structures with some atoms that are substantially inequivalent, such as in chains.

To address this issue, we have amended our code to handle an arbitrarily localized charge and used it to evaluate

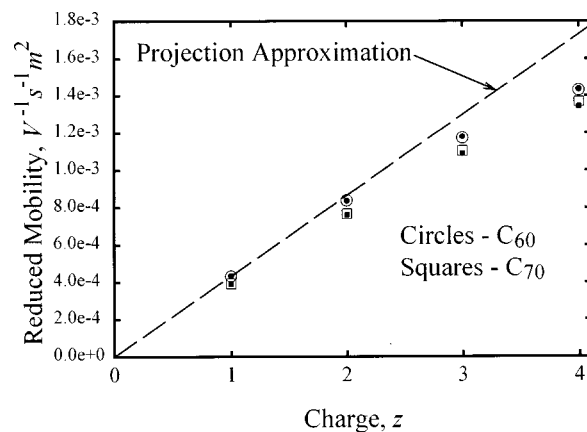


FIG. 5. Mobilities for the multiply charged C_{60}^{+z} and C_{70}^{+z} fullerene ions. Empty and filled symbols indicate the measurements⁶ and the results of our trajectory calculations, respectively. The dashed line⁶ corresponds to the projection approximation.

the mobilities for carbon chains under three different assumptions: (i) q (one elementary charge) on the central atom, (ii) q on one of the terminal atoms, and (iii) $0.5q$ on each terminal atom. The sign of the charge in this model is irrelevant. In Fig. 6, the resulting room-temperature mobilities are compared with those calculated under the assumption of fully delocalized charge. Regardless of the charge distribution, with increasing chain length the absolute magnitude of the effect first increases to a maximum at several atoms and then gradually tapers off. This is easy to rationalize considering the extremes of $n=1$ and $n \Rightarrow \infty$: in the first limit the charge is always localized on the same atom, whereas in the second limit the charge distribution is immaterial as the cluster is effectively neutral. For this general reason, the modulus of the effect of charge localization on mobility must maximize at a finite size for any cluster geometry, not only for the chains specifically considered here. It is clear that the concentration of charge on any one atom of the chain always causes a decrease in mobility. The localized charge deflects

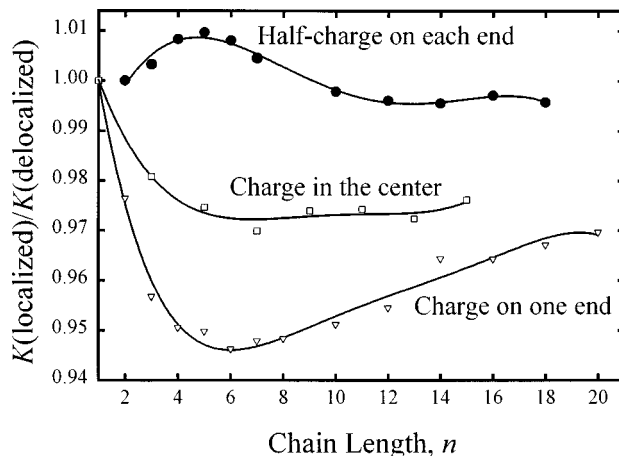


FIG. 6. Relative deviations of the mobilities for carbon chains calculated using various models for the localization of the extra charge from the values obtained under the assumption of the uniform charge localization. In all cases, the “fullerene” C–He elementary potential (Ref. 33) was employed. Lines are regressions through the data.

the He trajectories passing nearby strongly, and this apparently outweighs the weak deflection of all trajectories in the case of a uniform delocalization. However, the partial localization of the charge on several atoms may either decrease or increase the mobility. The latter may happen because the superposition of electric fields produced by different point charges creates regions with weak effective fields where the He trajectories are not influenced by the charge significantly. Such a region exists around the central atoms of short carbon chains assumed to bear $0.5q$ on each end (Fig. 6).

For any ion, the charge-induced dipole contribution to the total interaction potential with a buffer gas atom becomes dominant at long range. As the importance of the long-range potential increases with decreasing temperature, the localization of ionic charge should be particularly consequential for the low-temperature mobilities. This was brought out by repeating the calculations described above at 80 K. At this temperature, the mobilities for short ($n=5-10$) chains decrease by up to 7% (model i) and 18% (model ii) compared with a uniformly delocalized charge. In both cases, this is some three times the magnitude of the same effect at 298 K.

It is presently unclear how the ionic charge on real carbon chains (or other cluster isomers) is localized, and whether this is size dependent. However, the ad hoc incorporation of charge localization on top of our previously derived C-He potential does not bring the calculated mobilities for cationic carbon chains substantially closer to the measurements in any of the three versions considered. So it may be that the discrepancy is caused by effects beyond the scope of our model, such as the energy transfer into the internal degrees of freedom of polyatomic ions during inelastic collisions. The results of our ongoing research into the influence of charge localization on the mobilities of polyatomic ions will be reported elsewhere. The main findings at this juncture are that charge localization may have either positive or negative effect on the mobilities of cluster ions, and, when the charge is localized on a single atom, the effect is negative and can be substantial, particularly at low temperature.

VIII. CONCLUSIONS

We have demonstrated the capability of trajectory calculations using a realistic molecular potential between the ion and buffer gas atoms to evaluate the mobilities for polyatomic species with diverse sizes and shapes, including extremely elongated structures, isomers with concave surfaces, and geometries containing multiple holes. Specifically, carbon chains, monocyclic and bicyclic rings, graphite sheets, and fullerenes and their dimers have been investigated. For all these clusters, trajectory calculations employing the additive pairwise C-He potential, previously obtained by fitting the temperature dependence of the mobility of C_{60} in He, produce mobilities that are in a good agreement with the measurements over the 78–360 K temperature range. For example, at room temperature the agreement is three to ten times better than that with the values estimated using the hard-sphere projection approximation. This major improvement in the accuracy of mobility calculations in particular strengthens the case for assignment of the second fastest feature in the drift time distribution of carbon clusters in the

range of 30–70 atoms to graphite sheets.¹³ We also found that the large ($n=120-140$) fullerene cages have near-spherical shapes predicted by *ab initio* and semiempirical calculations, and hence are not prolate “buckytubes” as the projection approximation would suggest. The perfect agreement between the calculated and measured mobilities for multiply charged fullerene cages shows that our model treats the charge-induced dipole interaction appropriately and is also valid for multiply charged ions. However, the strong impact that charge localization could have on mobilities, particularly at lower temperatures, is revealed. Our results also show that the potential between helium and carbon clusters can to a good approximation be expressed as an additive pairwise potential, the Lennard-Jones form is a fair representation for the contribution from each C atom, and this contribution is at most weakly dependent on the cluster size and structure, even when the bonding is chemically different.

ACKNOWLEDGMENTS

We acknowledge Dr. G. B. Adams, Professor J. Cioslowsky, Dr. J. P. K. Doye, Professor J. M. L. Martin, Professor O. F. Sankey, Professor G. E. Scuseria, Dr. K. B. Shelimov, Dr. D. L. Strout, Professor D. J. Wales, and Professor M. Zerner for kindly providing us their optimized geometries for a variety of carbon clusters. We thank Dr. J. M. Hunter, Dr. Ph. Dugourd, R. R. Hudgins, and J. M. Tenenbaum for sharing with us their unpublished data for the mobilities of C_{120}^+ and anionic carbon chains. We are grateful to Dr. L. A. Pederson, Dr. V. A. Rassolov, and Professor M. A. Ratner for numerous insightful discussions, and to J. L. Fye for his help with the experimental work. This study was supported by the National Science Foundation (CHE-9618643) and the Army Research Office (DAAG 55-97-1-0133).

¹D. F. Hagen, *Anal. Chem.* **51**, 871 (1979).

²R. H. St. Louis and H. H. Hill, *Crit. Rev. Anal. Chem.* **21**, 321 (1990).

³G. von Helden, M. T. Hsu, P. R. Kemper, and M. T. Bowers, *J. Chem. Phys.* **95**, 3835 (1991).

⁴G. von Helden, P. R. Kemper, N. G. Gotts, and M. T. Bowers, *Science* **259**, 1300 (1993).

⁵G. von Helden, M. T. Hsu, N. G. Gotts, P. R. Kemper, and M. T. Bowers, *Chem. Phys. Lett.* **204**, 15 (1993).

⁶G. von Helden, M. T. Hsu, N. G. Gotts, and M. T. Bowers, *J. Phys. Chem.* **97**, 8182 (1993).

⁷G. von Helden, N. G. Gotts, W. E. Palke, and M. T. Bowers, *Int. J. Mass Spectrom. Ion Processes* **138**, 33 (1994).

⁸N. G. Gotts, G. von Helden, and M. T. Bowers, *Int. J. Mass Spectrom. Ion Processes* **149/150**, 217 (1995).

⁹J. M. Hunter, J. L. Fye, and M. F. Jarrold, *J. Chem. Phys.* **99**, 1785 (1993).

¹⁰J. M. Hunter, J. L. Fye, and M. F. Jarrold, *Science* **260**, 784 (1993).

¹¹J. M. Hunter, J. L. Fye, E. J. Roskamp, and M. F. Jarrold, *J. Phys. Chem.* **98**, 1810 (1994).

¹²J. M. Hunter, J. L. Fye, and M. F. Jarrold, *J. Phys. Chem.* **97**, 3460 (1993).

¹³K. B. Shelimov, J. M. Hunter, and M. F. Jarrold, *Int. J. Mass Spectrom. Ion Processes* **138**, 17 (1994).

¹⁴J. M. Hunter, J. L. Fye, N. M. Boivin, and M. F. Jarrold, *J. Phys. Chem.* **98**, 7440 (1994).

¹⁵D. E. Clemmer, J. M. Hunter, K. B. Shelimov, and M. F. Jarrold, *Nature (London)* **372**, 248 (1994).

¹⁶D. E. Clemmer and M. F. Jarrold, *J. Am. Chem. Soc.* **117**, 8841 (1995).

¹⁷K. B. Shelimov, D. E. Clemmer, and M. F. Jarrold, *J. Phys. Chem.* **99**, 11376 (1995).

¹⁸K. B. Shelimov and M. F. Jarrold, *J. Phys. Chem.* **99**, 17677 (1995).

¹⁹K. B. Shelimov, D. E. Clemmer, and M. F. Jarrold, *J. Chem. Soc. Dalton Trans.* **5**, 567 (1996).

- ²⁰G. von Helden, N. G. Gotts, P. Maitre, and M. T. Bowers, *Chem. Phys. Lett.* **227**, 601 (1994).
- ²¹J. L. Fye and M. F. Jarrold, *J. Phys. Chem. A* **101**, 1836 (1997).
- ²²G. von Helden, E. Porter, N. G. Gotts, and M. T. Bowers, *J. Phys. Chem.* **99**, 7707 (1995).
- ²³S. Lee, N. G. Gotts, G. von Helden, and M. T. Bowers, *Science* **267**, 999 (1995).
- ²⁴S. Lee, N. G. Gotts, G. von Helden, and M. T. Bowers, *J. Phys. Chem. A* **101**, 2096 (1997).
- ²⁵G. Von Helden, T. Wyttenbach, and M. T. Bowers, *Science* **267**, 1483 (1995).
- ²⁶Ph. Dugourd, R. R. Hudgins, D. E. Clemmer, and M. F. Jarrold, *Rev. Sci. Instrum.* **68**, 1122 (1997).
- ²⁷D. L. Strout, L. D. Book, J. M. Millam, C. Xu, and G. E. Scuseria, *J. Phys. Chem.* **98**, 8622 (1994).
- ²⁸D. L. Strout and G. E. Scuseria, *J. Phys. Chem.* **100**, 6492 (1994).
- ²⁹L. D. Book, C. Xu, and G. E. Scuseria, *Chem. Phys. Lett.* **222**, 281 (1994).
- ³⁰M. Krishnamurthy, J. A. de Gouw, V. M. Bierbaum, and S. R. Leone, *J. Phys. Chem.* **100**, 14908 (1996); M. Krishnamurthy, J. A. de Gouw, L. N. Ding, V. M. Bierbaum, and S. R. Leone, *J. Chem. Phys.* **106**, 530 (1997).
- ³¹S. J. Valentine, J. G. Anderson, A. D. Ellington, and D. E. Clemmer, *J. Phys. Chem. B* **101**, 3891 (1997); C. S. Hoaglund, Y. Liu, A. D. Ellington, M. Pagel, and D. E. Clemmer, *J. Am. Chem. Soc.* **119**, 9051 (1997).
- ³²E. Mack, Jr., *J. Am. Chem. Soc.* **47**, 2468 (1925).
- ³³M. F. Mesleh, J. M. Hunter, A. A. Shvartsburg, G. C. Schatz, and M. F. Jarrold, *J. Phys. Chem.* **100**, 16082 (1996); *J. Phys. Chem. A* **101**, 968 (1997).
- ³⁴A. A. Shvartsburg, R. R. Hudgins, Ph. Dugourd, and M. F. Jarrold, *J. Phys. Chem. A* **101**, 1684 (1997).
- ³⁵The same approach has been subsequently used to calculate the C₆₀ (neutral)-He scattering cross sections by A. Ruiz, J. Breton, and J. M. Gomez Llorente, *Chem. Phys. Lett.* **270**, 121 (1997).
- ³⁶J. Breton, J. Gonzalez-Platas, and C. Girardet, *J. Chem. Phys.* **99**, 4036 (1993).
- ³⁷M. F. Jarrold, *J. Phys. Chem.* **99**, 11 (1995).
- ³⁸E. A. Mason and E. W. McDaniel, *Transport Properties of Ions in Gases* (Wiley, New York, 1988).
- ³⁹In the zero field limit the mobility is rigorously proportional to the diffusion constant D : $K = De/k_B T$. As outlined in J. O. Hirschfelder, C. F. Curtiss, and R. B. Bird, *Molecular Theory of Gases and Liquids* (Wiley, New York, 1964), the diffusion constant also depends on the higher-order collision integrals such as $\Omega_{\text{avg}}^{(1,2)}$, $\Omega_{\text{avg}}^{(1,3)}$, and $\Omega_{\text{avg}}^{(2,2)}$. We have verified that the relative errors of truncating the expression at the $\Omega_{\text{avg}}^{(1,1)}$ term are below 0.01% for all clusters. The higher-order terms are negligible here because we operate in the Rayleigh limit, (Ref. 38) where the ions are much more heavier than the buffer gas atoms.
- ⁴⁰For fullerenes (Refs. 33 and 34) this correction to the temperature scale is negligible (< 1 K). The correction, however, rapidly increases with increasing drift velocity (which is inversely proportional to the collision integral) and may exceed 10 K for the smallest clusters studied here.
- ⁴¹L. A. Viehland and A. S. Dickinson, *Chem. Phys.* **193**, 255 (1995).
- ⁴²L. A. Viehland, A. S. Dickinson, and R. G. MacLagan, *Chem. Phys.* **211**, 1 (1996); W. K. Liu and A. S. Dickinson, *Mol. Phys.* **88**, 161 (1996).
- ⁴³S. N. Lin, G. W. Griffin, E. C. Horning, and E. E. Wentworth, *J. Chem. Phys.* **60**, 4994 (1974).
- ⁴⁴A. A. Shvartsburg and M. F. Jarrold, *Chem. Phys. Lett.* **86**, 261 (1996). Equations (2), (4), and (5) are correct as written here. The same formulas presented in the above reference are in error by a factor of two [Eqs. (2) and (4)] and $2/\pi$ [Eq. (5)].
- ⁴⁵We have acquired the data for $n = 7 - 10, 16, 18, 22, 24, 28, 30, 34, 36, 40$, and 46.
- ⁴⁶J. M. L. Martin and P. R. Taylor, *J. Phys. Chem.* **100**, 6047 (1996).
- ⁴⁷J. M. L. Martin, J. El-Yazal, and J. P. Francois, *Chem. Phys. Lett.* **252**, 9 (1996).
- ⁴⁸J. Hutter and H. P. Luthi, *J. Chem. Phys.* **101**, 2213 (1994).
- ⁴⁹J. Hutter, H. P. Luthi, and F. Diederich, *J. Am. Chem. Soc.* **116**, 750 (1994).
- ⁵⁰T. F. Giesen, A. Van Orden, H. J. Hwang, R. S. Fellers, R. A. Provencal, and R. J. Saykally, *Science* **265**, 756 (1994).
- ⁵¹H. J. Hwang, A. Van Orden, K. Tanaka, E. W. Kuo, J. R. Heath, and R. J. Saykally, *Mol. Phys.* **79**, 769 (1993).
- ⁵²D. A. Plattner and K. N. Houk, *J. Am. Chem. Soc.* **117**, 4405 (1995).
- ⁵³K. Raghavachari, D. L. Strout, G. K. Odom, G. E. Scuseria, J. A. Pople, B. G. Johnson, and P. M. W. Gill, *Chem. Phys. Lett.* **214**, 357 (1993).
- ⁵⁴K. Raghavachari, B. Zhang, J. A. Pople, B. G. Johnson, and P. M. W. Gill, *Chem. Phys. Lett.* **220**, 385 (1994).
- ⁵⁵J. M. L. Martin, J. P. Francois, R. Gijbels, and J. Almlof, *Chem. Phys. Lett.* **187**, 367 (1991).
- ⁵⁶J. M. L. Martin, J. El-Yazal, and J. P. Francois, *Chem. Phys. Lett.* **248**, 345 (1996).
- ⁵⁷J. M. L. Martin, J. El-Yazal, and J. P. Francois, *Chem. Phys. Lett.* **255**, 7 (1996).
- ⁵⁸J. D. Watts and R. J. Bartlett, *Chem. Phys. Lett.* **190**, 19 (1992).
- ⁵⁹Martin *et al.* (Ref. 47) found that the lowest energy isomers for small neutral carbon rings are not circular, but feature strongly alternating bond angles. The calculated mobilities of these geometries ($n = 7 - 18$) are slightly (within 1.5%) below those of our model structures.
- ⁶⁰K. B. Shelimov (private communication).
- ⁶¹All MNDO-optimized coordinates used in this paper have been scaled by 0.9884. This scaling, necessary to match the MNDO geometry for C₆₀ fullerene with the experimental structure, has been applied to all MNDO geometries for carbon clusters in our preceding work (Refs. 33 and 34).
- ⁶²D. L. Strout, R. L. Murry, C. Xu, W. C. Eckhoff, G. K. Odom, and G. E. Scuseria, *Chem. Phys. Lett.* **214**, 576 (1993).
- ⁶³Measurement is from J. M. Hunter and M. F. Jarrold (unpublished results).
- ⁶⁴G. B. Adams, O. F. Sankey, J. B. Page, M. O'Keeffe, and D. A. Drabold, *Science* **256**, 1792 (1992).
- ⁶⁵D. Bakowies and W. Thiel, *J. Am. Chem. Soc.* **113**, 3704 (1991).
- ⁶⁶G. E. Scuseria, in *Buckminsterfullerenes*, edited by W. E. Billups and M. A. Ciufolini (VCH Weinheim, 1993), p. 103.
- ⁶⁷J. M. Hunter and M. F. Jarrold, *J. Am. Chem. Soc.* **117**, 10317 (1995).
- ⁶⁸J. R. Heath and R. J. Saykally, *J. Chem. Phys.* **94**, 1724 (1991).
- ⁶⁹A. Van Orden, H. J. Hwang, E. W. Kuo, and R. J. Saykally, *J. Chem. Phys.* **98**, 6678 (1993).
- ⁷⁰Ph. Dugourd, R. R. Hudgins, J. M. Tenenbaum, and M. F. Jarrold (to be published).
- ⁷¹Von Helden *et al.* (Ref. 6) proposed that the decrease of mobility with increasing charge is in part due to the expansion of multiply charged fullerene cages by Coulombic repulsion. To check this possibility, we have calculated the mobilities for optimized geometries of C₆₀ fullerene in the (+1) charge state [R. D. Bendale, J. F. Stanton, and M. C. Zerner, *Chem. Phys. Lett.* **194**, 467 (1992)], and (+2) and (+4) charge states [J. Cioslowsky, S. Patchkovskii, and W. Thiel, *Chem. Phys. Lett.* **248**, 116 (1996)]. In all cases, the difference in mobility from that of the ideal I_h structure is under 0.3%, which is within the experimental error margin.